

# Supplementary Material

## Functional role of lanthanides in enzymatic activity and transcriptional regulation of PQQ-dependent alcohol dehydrogenases in *Pseudomonas putida* KT2440

Matthias Wehrmann<sup>a</sup>, Patrick Billard<sup>b,c</sup>, Audrey Martin-Meriadec<sup>b,c</sup>, Asfaw Zegeye<sup>b,c</sup>, Janosch Klebensberger<sup>a#</sup>

### ***Specific chemicals***

Pyrrroloquinoline quinone (PQQ) disodium salt, 2,6-dichlorophenol indophenol sodium salt and 5-fluorouracil were purchased from Sigma-Aldrich. Phenazine methosulfate was obtained from Santa Cruz Biotechnology. Lanthanum, praseodymium, cerium, neodymium, samarium, gadolinium, terbium, erbium, ytterbium, scandium and yttrium were obtained as chloride salts from Sigma-Aldrich or Santa Cruz Biotechnology. All liquid chemicals were purchased from VWR Chemicals, Merck or Sigma-Aldrich in purities of  $\geq 99.0\%$ .

### ***Construction of plasmids***

The *pedE* and *pedH* genes of *Pseudomonas putida* KT2440 were amplified from genomic DNA using Q5 Hot-Start DNA polymerase (New England BioLabs) and primer pairs *MWH11/MWH12* and *MWH13 /MWH14* (**Table S1**). The primers harbored a C-terminal 6xHis-tag and a > 15 bp homology to the insertion sites in plasmid pJeM1 on each site. The *eGFP* gene in plasmid pJeM1 was excised using NdeI and HindIII and replaced with the purified PCR products *via* the one-step isothermal assembly as described by Gibson *et al.* (1). The constructs were subsequently transformed into *E. coli* BL21 (DE3) and the correctness of the cloned genes was verified by Sanger sequencing (GATC Biotech).

For construction of the integration vector pMW43, pJOE6261.2 was digested with BamHI. Additionally the 1000 bp regions up- and downstream of the gene cluster *pqqABCDE* were amplified from genomic DNA of *P. putida* KT2440 using primer pairs MWH34/MWH35 and MWH36/MWH37. The three fragments were joined together using the one-step isothermal assembly as described by Gibson *et al.* (1). The constructs were subsequently transformed into *E. coli* BL21 (DE3) and the correctness of the plasmid was confirmed by Sanger sequencing.

For quantifying the transcriptional activities of *pedE* and *pedH* *in vivo* plasmids pUC18-mini-Tn7-*pedE-lux-Gm* and pUC18-mini-Tn7T-*pedH-lux-Gm* were constructed (2). The DNA regions encompassing the promoter from *pedE* and *pedH* genes were amplified by PCR (Phusion DNA polymerase, Fermentas) using the primer pairs p2674-FSac/p2674-RPst and p2679-FSac/p2679-RPst (**Table S1**), respectively. PCR products were digested with SacI and PstI and cloned upstream the *luxCDABE* operon hosted by plasmid pUC18-mini-Tn7T-Gm-lux. The resulting mini-Tn7 constructs were co-electroporated with the helper plasmid pTNS2 into KT2440 and mutant strains  $\Delta pedE$  and  $\Delta pedH$  (2, 3). Proper chromosomal integration of Tn7 elements was verified by PCR using Pput-*glmSDN* and PTn7R primers as described previously (2).

**Table 1:** Strain, plasmids, and primer used in the study

Strains	Relevant features
KT2440	Wildtype strain of <i>Pseudomonas putida</i> (ATCC 47054)
KT2440*	KT2440 with a markerless deletion of <i>upp</i>   Parent strain for deletion mutants (4)
$\Delta pedH$	$\Delta upp$ with a markerless mutation of <i>pedH</i> (5)
$\Delta pedE$	$\Delta upp$ with a markerless deletion of <i>pedE</i> (5)
$\Delta pedE\Delta pedH$	$\Delta upp$ with a markerless deletion of <i>pedE</i> and <i>pedH</i> (5)
$\Delta pqq$	$\Delta upp$ with a markerless deletion of <i>pqqABCDE</i> (this study)
<i>E. coli</i> BL21 (DE3)	$F^- ompT gal dcm lon hsdS_B(r_B^- m_B^-) \lambda(DE3 [lacI lacUV5-T7 gene 1 ind1 sam7 nin5])$
<i>E. coli</i> DH5 $\alpha$	<i>fhuA2 lac(del)U169 phoA glnV44 <math>\Phi</math>80' lacZ(del)M15 gyrA96 recA1 relA1 endA1 thi-1 hsdR17</i>
<b>Plasmids</b>	



vector pMW43 harboring the up- and downstream regions of the target gene cluster *pqqABCDE* was constructed and transformed into *P. putida* KT2440  $\Delta upp$  (referred to as KT2440\* within this manuscript). Kanamycin (Kan) resistant and 5-fluorouracil (5-FU) sensitive clones were selected on LB agar plates containing 40  $\mu\text{g ml}^{-1}$  Kan and one of these was incubated in LB medium at 30°C for 24 h. The cell suspension was subsequently plated on M9 minimal agar plates containing 20 mM glucose and 20  $\mu\text{g ml}^{-1}$  5-FU. Clones that carried the desired gene deletion were identified by colony PCR of the 5-FU<sup>r</sup> Kan<sup>s</sup> clones using primer pair MWH34/MWH37.

### ***Expression and purification of PedE and PedH***

For production and purification of C-terminally His-tagged PedE and PedH, cells of *E. coli* BL21 (DE3) carrying plasmid pMW09 or pMW10 were grown in liquid LB medium supplemented with kanamycin and 1 mM CaCl<sub>2</sub> at 37°C and 180 rpm. When cells reached an OD<sub>600</sub> of  $\geq 0.5$  (Eppendorf, BioPhotometer) protein production was induced by addition of 0.2% [w/v] rhamnose and the medium was additionally supplemented with 0.6  $\mu\text{M}$  pyrroloquinoline quinone (PQQ). Subsequently, cultures were shifted to 16°C and incubated at 180 rpm (HT Aerotron, Infors). After 16 h, cells were harvested by centrifugation (6000  $\times g$ , 15 min, 4°C, Centrifuge 5810 R, Eppendorf), lysed by treatment with 1 $\times$  Bugbuster solution (50 mM Tris-HCl pH 7.5 and 300 mM NaCl) supplemented with DNase (5  $\mu\text{g/ml}$ ) and lysozyme (5  $\mu\text{g/ml}$ ) and cell debris was removed by centrifugation (20000  $\times g$ , 20 min, 4°C, Centrifuge 5424 R, Eppendorf). His-tagged PedE and PedH were purified from the cell-free extracts using affinity chromatography (His GraviTrap Talon<sup>®</sup> columns, GE Healthcare). For this 2 – 10 ml cell-free extract was loaded on a column, washed with 10 ml wash buffer (50 mM Tris-HCl pH 7.5, 300 mM NaCl, 5 mM imidazole) and eluted with 3 ml elution buffer (50 mM Tris-HCl pH 7.5, 300 mM NaCl, 150 mM Imidazole). Subsequently, excess

ions were diluted 10 000-fold by dialysis with 50 mM Tris-HCl buffer pH 7.5. Protein purity was determined by visual inspection on SDS-PAGE (**Fig. S1**) and protein concentration was determined based on absorbance at 280 nm using a NanoDrop 2000 device. Eventually, enzymes were stored at -80°C as 1 mg ml<sup>-1</sup> stock in 50 mM Tris HCl pH 7.5 containing 1 mg ml<sup>-1</sup> bovine serum albumin (BSA) for stabilization.

### ***Amine source dependency of the enzymatic assay***

The optimal amine source and concentration was determined by using the enzyme activity assay described in materials and methods omitting imidazole in the presence of different amine sources. These included the commonly used amine sources ammonium chloride (45 mM) and ethylamine (5 mM) at reported concentrations as well as imidazole (6, 7). As imidazole gave an about 8-fold higher activity as ammonium chloride and an about 12-fold higher activity compared to ethylamine the ideal imidazole concentration was determined (**Fig. S5**). Therefore, the enzymatic assay was carried out at various imidazole concentrations and it was found that highest activities were measured for both PedE and PedH at concentrations above 25 mM (**Fig. S6**). For better visualization, the activities at varying imidazole concentrations were fitted by the least square method to a one site binding model based on the assumption that at  $v_{max}$  100% of the enzyme concentration is present associated with imidazole:

$$v_0 = \frac{v_{max} \times [im]}{K_D + [im]}$$

Where [im] is the imidazole concentration,  $v_0$  is the specific enzymatic activity at a certain imidazole concentration [im],  $v_{max}$  is the maximal specific enzyme activity and  $K_D$  is the dissociation constant.

### ***Phenazine methosulfate (PMS) dependency of the enzymatic assay***

The effect of the PMS concentration on the enzymatic assay was determined using 100 mM Tris HCl pH 8; 150  $\mu$ M 2,6-dichlorophenol indophenol; 25 mM imidazole; 1  $\mu$ M PrCl<sub>3</sub>; 1  $\mu$ M PQQ; 12.5  $\mu$ L substrate and 3  $\mu$ g/ml PedH at various PMS concentrations. The highest activities are observed when using 500  $\mu$ M or more PMS (**Fig. S7**).

### ***Pyrroloquinoline quinone (PQQ) affinity of the enzymes***

The optimal PQQ concentration for each enzyme was identified by using the enzymatic assay described in material and methods at varying PQQ concentrations. Highest activities were observed with 50  $\mu$ M PQQ for PedE and with 0.5 and 1  $\mu$ M PQQ for PedH (**Fig. S8**). For comparison purposes a dissociation constant  $K_D$  was calculated by least-square analysis of the enzyme activities fitted with a one site binding model based on the assumption that at  $v_{max}$  100% of the enzyme concentration is present in PQQ bound form:

$$v_0 = \frac{v_{max} \times [PQQ]}{K_D + [PQQ]}$$

Where [PQQ] is the PQQ concentration,  $v_0$  is the specific enzymatic activity at a certain PQQ concentration [PQQ],  $v_{max}$  is the maximal specific enzyme activity and  $K_D$  is the dissociation constant.

### ***Metal binding affinity of the enzymes***

To test the metal binding affinities of PedE and PedH, a similar set-up as described in material and methods was used omitting CaCl<sub>2</sub> for PedE or PrCl<sub>3</sub> for PedH in the assay solution. Various concentrations of different metals were added prior to incubation at 30°C. These included LaCl<sub>3</sub>, CeCl<sub>3</sub>, PrCl<sub>3</sub> and CaCl<sub>2</sub>. To allow comparison of different enzymes and metals, a dissociation

constant  $K_D$  was calculated by least-square analysis of the enzyme activities fitted with a one site binding model based on the assumption that at  $v_{max}$  100% of the enzyme concentration is present in metal bound form:

$$v_0 = \frac{v_{max} \times [M]}{K_D + [M]}$$

Where  $[M]$  is the metal concentration,  $v_0$  is the specific enzymatic activity at a certain metal concentration  $[M]$ ,  $v_{max}$  is the maximal specific enzyme activity with a given metal  $M$  and  $K_D$  is the dissociation constant.

## References

1. **Gibson DG, Young L, Chuang R-Y, Venter JC, Hutchison C a, Smith HO.** 2009. Enzymatic assembly of DNA molecules up to several hundred kilobases. *Nat Methods* **6**:343–345 doi:10.1038/nmeth.1318.
2. **Choi K-H, Gaynor JB, White KG, Lopez C, Bosio CM, Karkhoff-Schweizer RR, Schweizer HP.** 2005. A Tn7-based broad-range bacterial cloning and expression system. *Nat Methods* **2**:443–448 doi:10.1038/nmeth765.
3. **Choi K-H, Kumar A, Schweizer HP.** 2006. A 10-min method for preparation of highly electrocompetent *Pseudomonas aeruginosa* cells: Application for DNA fragment transfer between chromosomes and plasmid transformation. *J Microbiol Methods* **64**:391–397 doi:10.1016/j.mimet.2005.06.001.
4. **Graf N, Altenbuchner J.** 2011. Development of a method for markerless gene deletion in *Pseudomonas putida*. *Appl Environ Microbiol* **77**:5549–5552 doi:10.1128/AEM.05055-11.
5. **Mückschel B, Simon O, Klebensberger J, Graf N, Rosche B, Altenbuchner J, Pfannstiel J,**

- Huber A, Hauer B.** 2012. Ethylene glycol metabolism by *Pseudomonas putida*. *Appl Environ Microbiol* **78**:8531–9 doi:10.1128/AEM.02062-12.
6. **Jeske M, Altenbuchner J.** 2010. The *Escherichia coli* rhamnose promoter rhaP BAD is in *Pseudomonas putida* KT2440 independent of Crp–cAMP activation. *Appl Microbiol Biotechnol* **85**:1923–1933 doi:10.1007/s00253-009-2245-8.
7. **Chattopadhyay A, Förster-Fromme K, Jendrossek D.** 2010. PQQ-dependent alcohol dehydrogenase (QEDH) of *Pseudomonas aeruginosa* is involved in catabolism of acyclic terpenes. *J Basic Microbiol* **50**:119–24 doi:10.1002/jobm.200900178.
8. **Anthony C, Zatman LJ.** 1964. The microbial oxidation of methanol. 2. The methanol-oxidizing enzyme of *Pseudomonas* sp. M 27. *Biochem J* **92**:614–21.

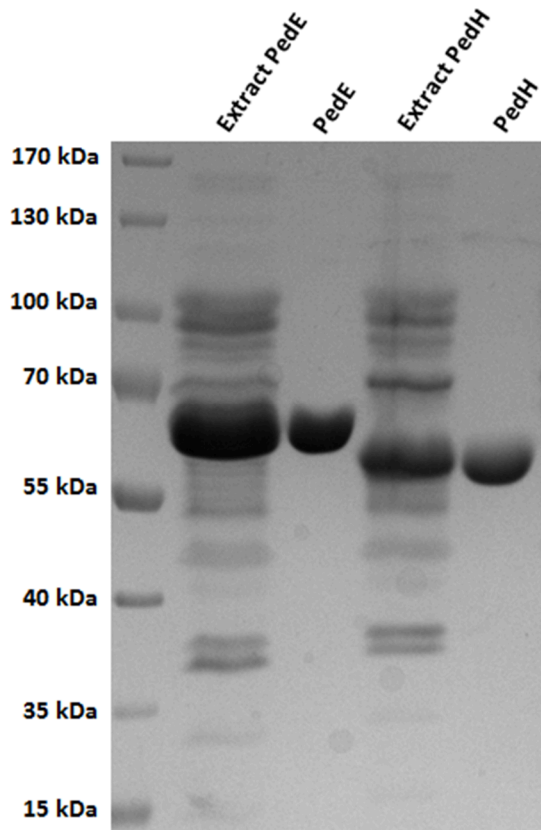
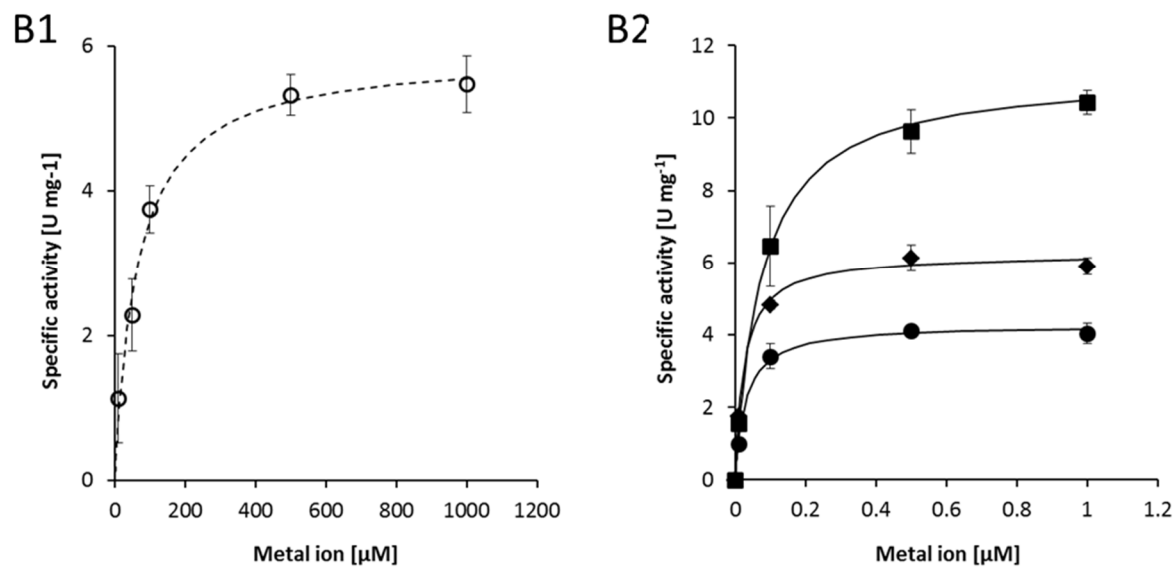
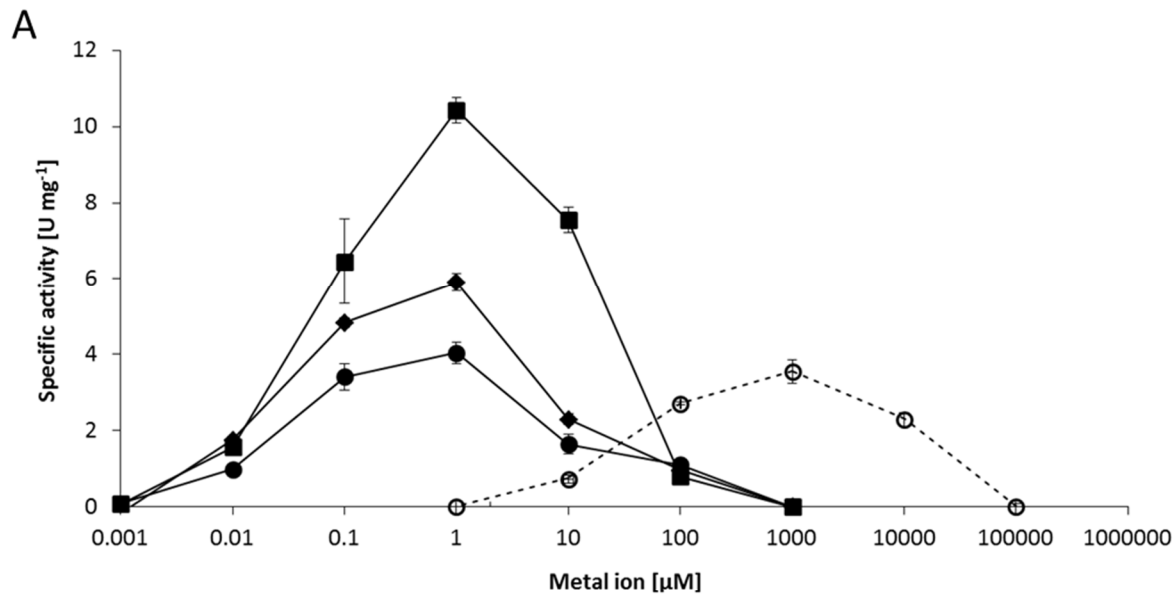


**Fig. S1:** SDS-PAGE analysis of PedE and PedH production. 10  $\mu$ l cell extract or 20  $\mu$ g of purified protein were loaded per lane.



FIG

**Fig. S2: A)** Specific activities of PedE (*dashed line*) or PedH (*solid lines*) in presence of different ion concentrations of  $\text{Ca}^{2+}$  (*empty circles*),  $\text{La}^{3+}$  (*dark circles*),  $\text{Ce}^{3+}$  (*black diamonds*) or  $\text{Pr}^{3+}$  (*black squares*). **B)** Specific activities of PedE (**B1**) or PedH (**B2**) at different metal concentrations. Data were fitted to a one site binding model by least square analysis and affinity constants of PedE for  $\text{Ca}^{2+}$  ( $K_D = 64 \mu\text{M}$ ) and PedH for  $\text{Pr}^{3+}$  ( $K_D = 75 \text{ nM}$ ),  $\text{Ce}^{3+}$  ( $K_D = 25 \text{ nM}$ ) and  $\text{La}^{3+}$  ( $K_D = 30 \text{ nM}$ ) were calculated.

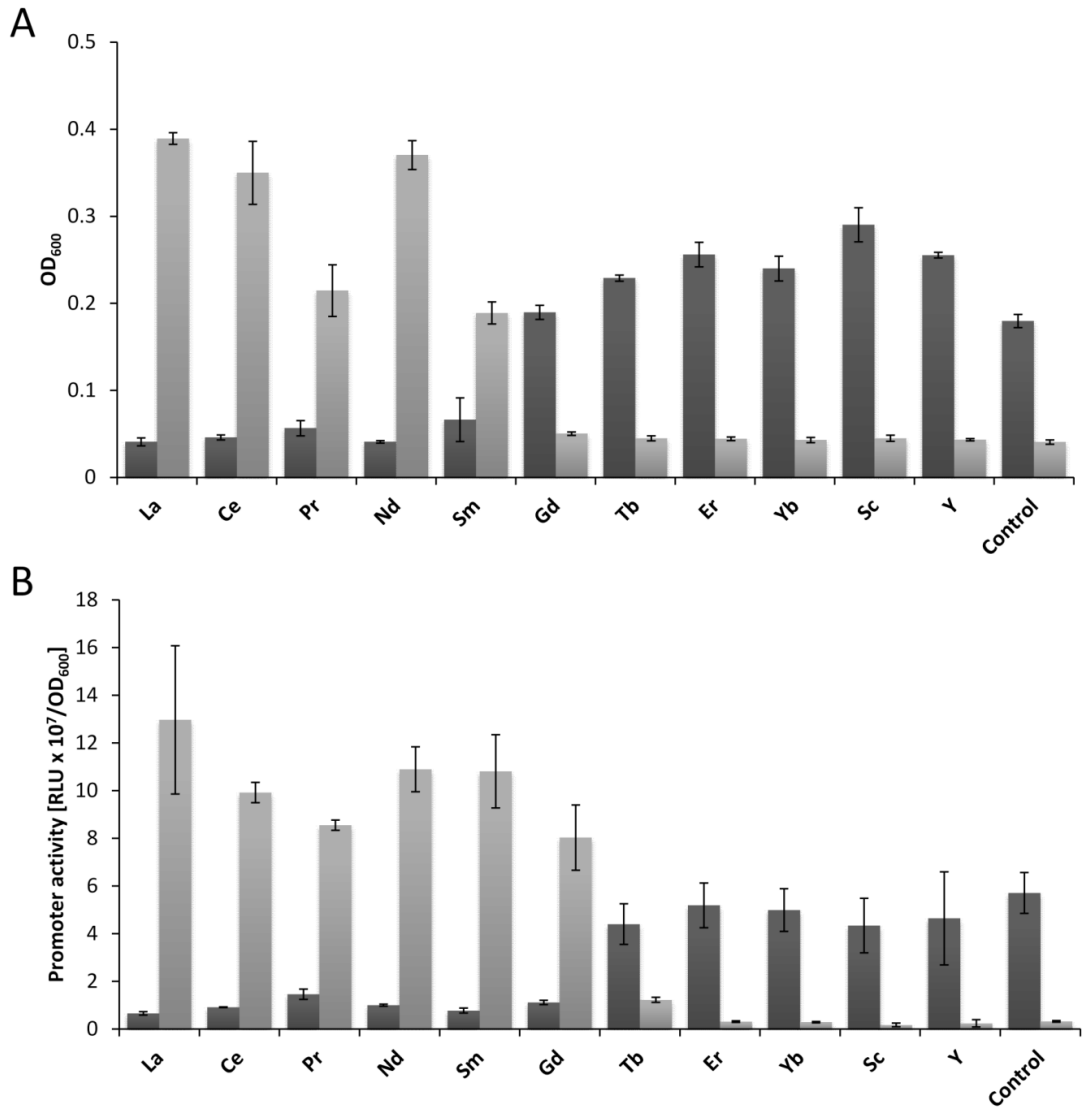


**Fig. S3:** (A) Growth of strains  $\Delta pedE$  (light grey bars) and  $\Delta pedH$  (dark grey bars) after incubation for 24 h at 30°C in liquid M9 minimal medium containing 5 mM of 2-phenylethanol as source of carbon and energy supplemented with 20  $\mu$ M of different rare earth metals. (B) Transcription from the *pedE* promoter (dark grey bars) and *pedH* promoter (light grey bars) in strain KT2440\* in liquid MP minimal medium containing 1 mM of 2-phenylethanol supplemented with 20  $\mu$ M of different rare earth metals. Transcriptional levels are presented as responsive light units (RLU) normalized to OD<sub>600</sub>. Bars represent the mean of three biological replicates and error bars show the corresponding standard deviation.

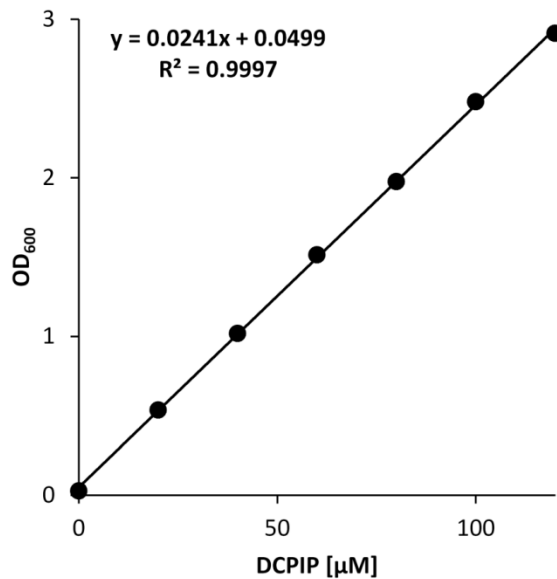


**Fig. S4:** Extinction coefficient of 2,6-dichlorophenolindophenol (DCPIP) was calculated to be  $\epsilon = 24.1 \text{ cm}^{-1} \text{ mM}^{-1}$  from linear relation between absorbance at 600 nm ( $\text{OD}_{600}$ ) and DCPIP concentration.

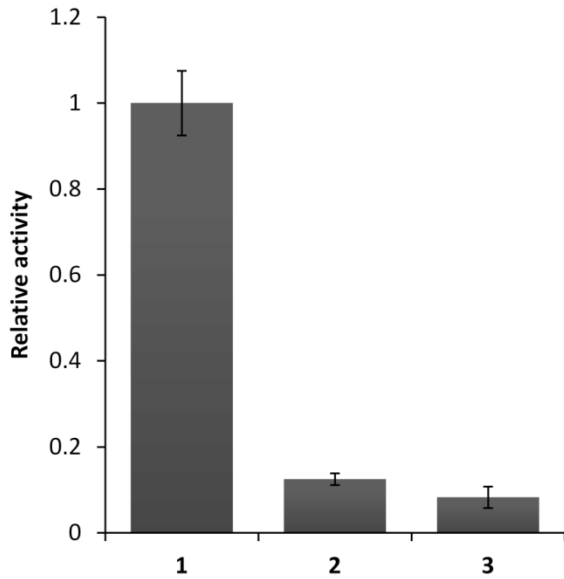


**Figure S5:** Relative activity of PedE with 10 mM ethanol as substrate in presence of 25 mM imidazole (**1**), 45 mM ammonium chloride (**2**) or 5 mM ethylamine (**3**). Activity is 8- respectively 12-times higher with 25 mM imidazole compared to 45 mM ammonium chloride or 5 mM ethylamine.

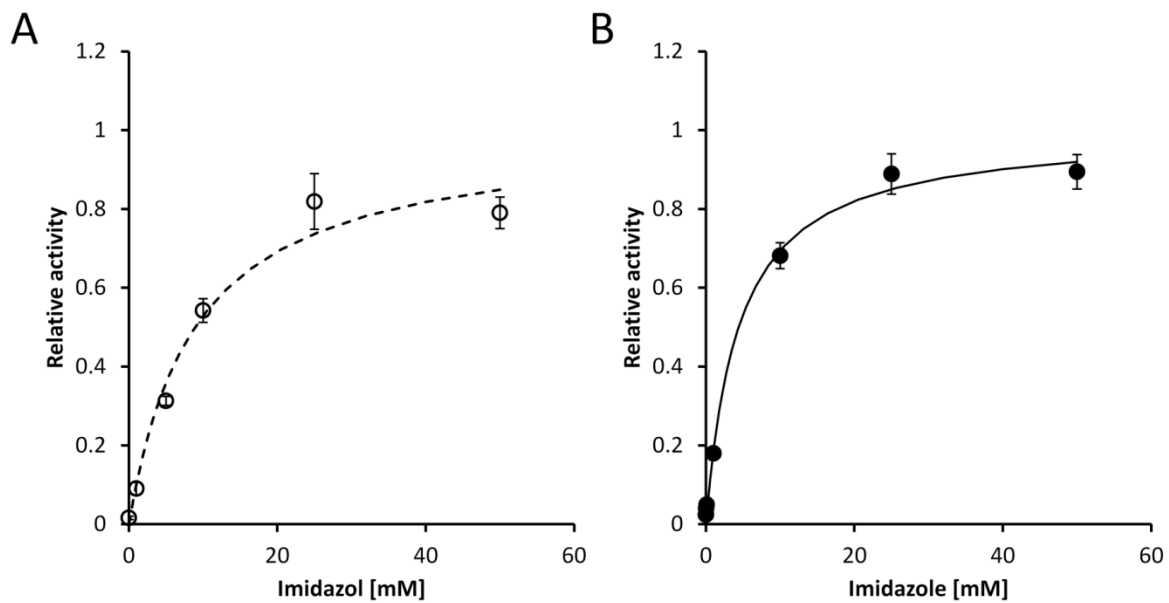


**Fig. S6:** Relative activities of PedE (A) and PedH (B) with 10 mM ethanol as substrate in presence of increasing concentrations of imidazole. For better visualization, data were fitted (*dashed line* for PedE and *continuous line* for PedH) to a one site binding model by nonlinear regression.

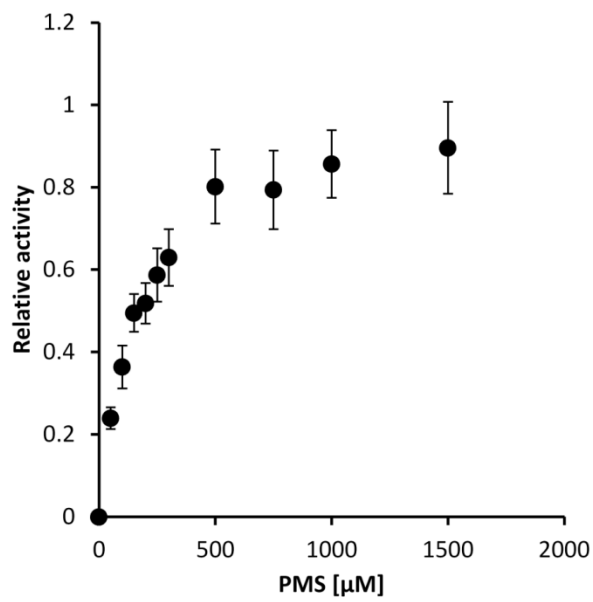


**Fig. S7:** Relative activity of PedH with 10 mM ethanol as substrate in presence of varying phenazine methosulfate (PMS) concentrations. 500  $\mu\text{M}$  PMS were determined to be sufficient for robust results by visual inspection.

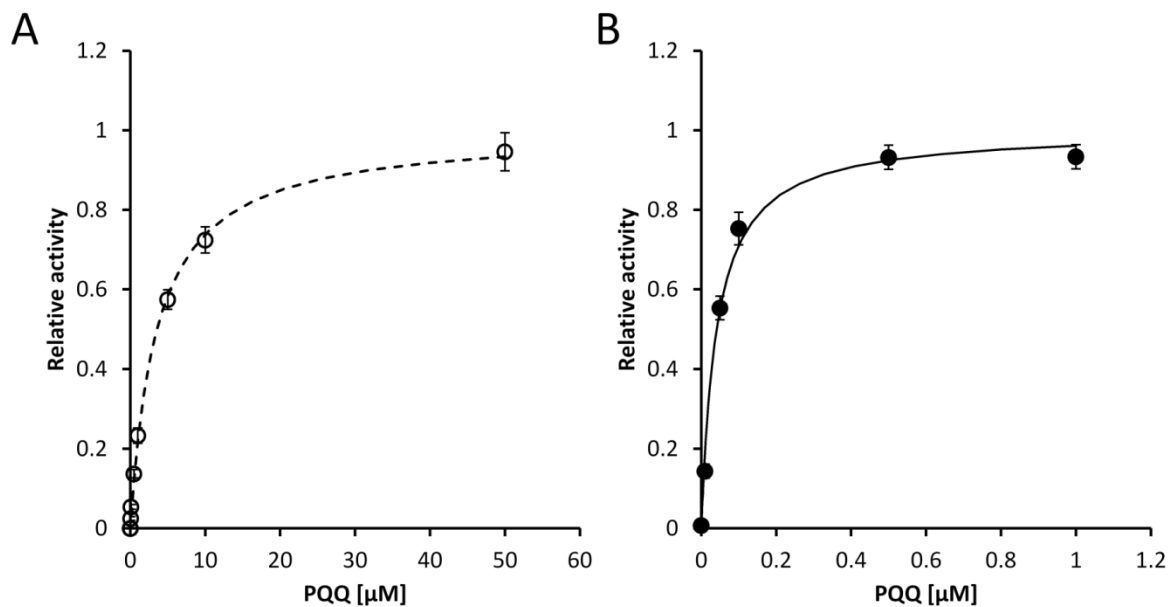


**Fig. S8:** Relative activities of PedE (**A**) and PedH (**B**) with 10 mM ethanol as substrate in presence of increasing concentrations of pyrroloquinoline quinone (PQQ). Dashed (PedE) or continuous (PedH) lines represent nonlinear fit to a one site binding model.  $K_D$  values were calculated to be 3.5  $\mu\text{M}$  for PedE and 41 nM for PedH.

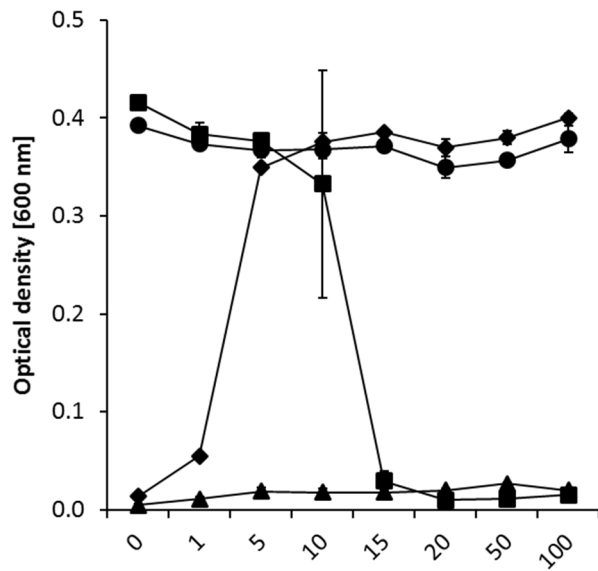


**Fig. S9:** Growth of KT2440\* (black circles),  $\Delta upp\Delta pedE$  (black diamonds),  $\Delta upp\Delta pedH$  (black squares) and  $\Delta upp\Delta pedE\Delta pedH$  (black triangles) in liquid MP medium with 5 mM of 2-phenylethanol in the presence of different La<sup>3+</sup> concentrations. Growth was determined as the optical density at 600 nm after incubation at 30°C for 48 h. Data are presented as the mean values from biological triplicates and error bars represent the corresponding standard deviation.